Real-Time, Nonlinear Control of a Constrained, Nonminimum-Phase Process

Joshua M. Kanter and Warren D. Seider
Dept. of Chemical Engineering, University of Pennsylvania, Philadelphia, PA 19104

Masoud Soroush
Dept. of Chemical Engineering, Drexel University, Philadelphia, PA 19104

This article presents the first real-time implementation of a recently-developed model-based control method on a pilot-scale, multivariable, liquid-level process that exhibits inverse response and whose actuators can be saturated. Issues in real-time implementation of the control method are discussed, as well as a controller tuning procedure. Two model-based controllers are implemented: one is derived using the process outputs; the other is derived using auxiliary outputs. Servo and regulatory responses presented show the differences in the performance of the two controllers. In real time, one of the model-based controllers eliminates inverse response in one controlled output at the expense of yielding a larger inverse response in the other controlled output. This inverse-response elimination is a real-time validation of the linear and nonlinear theoretical results reported in the systems literature.

Introduction

During the past 20 years, many advances have been made in nonlinear model-based control, mainly in the frameworks of model-predictive and differential-geometric control. In model-predictive control, the controller action is the solution to a constrained optimization problem that is solved on-line. In contrast, differential-geometric control is a direct synthesis approach in which the controller is derived by requesting a desired closed-loop response in the absence of input constraints. While in model-predictive control, nonminimum-phase behavior is handled simply by increasing prediction horizons, in differential geometric control, special treatment is needed.

Differential-geometric controllers were initially developed for unconstrained, minimum-phase (MP) processes. During the past two decades, these controllers were extended to unconstrained, nonminimum-phase (NMP), nonlinear processes. The resulting controllers include those developed by Kravaris and Daoutidis (1990), Isidori and Byrnes (1990), Isidori and Astolfi (1992), Wright and Kravaris (1992), van der Schaft (1992), Isidori (1995), Chen and Paden (1996), Devasia et al. (1996), Doyle III et al. (1996), McLain et al. (1996), Hunt and Meyer (1997), Niemiec and Kravaris (1998), Kravaris et al. (1998), and Devasia (1999). Most of these controllers are applicable only to single-input single-output, NMP processes. Although controllers of Niemiec and Kravaris (1998), Isidori and Byrnes (1990), Isidori and Astolfi (1992), van der Schaft (1992), Chen and Paden (1996), Hunt and Meyer (1997), Devasia et al. (1996), Devasia (1999), and Isidori (1995) are applicable to multi-input, multi-output (MIMO), NMP processes, either sets of partial differential equations must be solved (Isidori and Byrnes, 1990; Isidori and Astolfi, 1992; van der Schaft, 1992), or the controllers are applicable to a very limited class of processes (Chen and Paden, 1996; Hunt and Meyer, 1997; Devasia et al., 1996; Devasia, 1999; Isidori, 1995). Recently, a differential-geometric control law was developed by Kanter et al. (2002) for stable, nonlinear processes with input constraints and deadtimes, whether the delay-free part of the process is nonminimum- or minimum-phase. This control law minimizes the error between the delay-free controlled outputs and their reference trajectories. Implementation of the control law requires solving a simple constrained-optimization problem on-line.

This article presents a real-time implementation of the control law in Kanter et al. (2002) on a pilot-scale, multivari-

Correspondence concerning this article should be addressed to M. Soroush.

able, liquid-level process in the Process Control Laboratory at the Dept. of Chemical Engineering of the University of Delaware (Gatzke et al., 1999). Issues in real-time implementation of the control method are discussed, and a controller tuning procedure is presented. The process, which has four tanks and two pumps, exhibits inverse response. Cross-feeding to the tanks results in a movable process zero, which depends on the fraction of the pump effluents sent to two of the tanks (Johansson and Nunes, 1998). Two controllers are developed and implemented, one derived using the process outputs and the other derived using two auxiliary outputs. Servo and regulatory responses are presented to compare the performance of the two controllers.

Some preliminaries are given in the next section followed by a description of the liquid-level process. Two nonlinear, model-based controllers are synthesized and a controller tuning procedure is presented, and the closed-loop performance of the controllers and their computational loads are compared.

Preliminaries

For the nonminimum-phase, multivariable, liquid-level process, two model-based controllers are developed and implemented. While the error-feedback control law presented by Kanter et al. (2002) is used to design both controllers, the second uses auxiliary outputs, constructed using the method of Niemiec and Kravaris (1998). For completeness, the method is reviewed here.

Requirements for equivalent outputs

Consider a nonminimum-phase process with a mathematical model in the form

$$\left.\begin{aligned} &\frac{dx}{dt} = f(x) + g(x)u, \qquad x(0) = x_0 \\ &y_i = h_i(x),\, i = 1, \ldots, m \end{aligned}\right\} \tag{1}$$

where $x\mathrm{x} = [x_1 \ \cdots \ x_n]^T \in X$ is the vector of state variables, $u = [u_1 \ \cdots \ u_m]^T \in \boldsymbol{U}$ is the vector of manipulated inputs, $y = [y_1 \ \cdots \ y_m]^T$ is the vector of controlled outputs, $f(.)$ and $g(.)$ are smooth vector fields on X, and $h_1(.), \cdots, h_m(.)$ are smooth functions on X. Here $X \subset \Re^n$ is a connected open set that includes x_{ss} and x_0; $\boldsymbol{U} = \{u | u_{l_i} \le u_i \le u_{h_i},\ i = 1, \cdots, m\} \subset \Re^m$ that includes u_{ss}; $u_{l_1}, \cdots, u_{l_m}, u_{h_1}, \cdots, u_{h_m}$ are real scalars; and (x_{ss}, u_{ss}) denotes the nominal steady-state (equilibrium) pair of the process; that is, $f(x_{ss}) + g(x_{ss})u_{ss} = 0$.

The relative order (degree) of a controlled output y_i, is denoted by r_i, where r_i is the smallest integer for which $[L_{g_1} L_f^{r_i - 1} h_i(x) \cdots L_{g_m} L_f^{r_i - 1} h_i(x)] \not\equiv [0 \ \cdots \ 0]$; in practice, these are finite. The characteristic (decoupling) matrix of the process, $\mathcal{C}(x)$, an $m \times m$ matrix with $\mathcal{C}_{ij} = L_{g_j} L_f^{r_i - 1} h_i(x)$, is assumed to be nonsingular for all x.

For a process that exhibits nonminimum-phase behavior, auxiliary outputs are determined

$$y_{A_i} = h_{A_i}(x), \qquad i = 1, \cdots, m \tag{2}$$

where $h_{A_1}(.), \cdots, h_{A_m}(.)$ are smooth functions, which satisfy the following conditions:

(1) Each auxiliary output y_{A_i} must have a relative order (degree) equal to r_i; that is, the relative order of the ith auxiliary output must equal that of the ith output.

(2) The characteristic (decoupling) matrix of the process, expressed in terms of the auxiliary outputs, an $m \times m$ matrix with $\mathcal{C}_{A_{ij}} = L_{g_j} L_f^{r_i - 1} h_{A_i}(x)$, must be nonsingular for all x.

(3) The auxiliary outputs must be statically equivalent to the process outputs: $h_{A_i}(x_{ss}) = h_i(x_{ss})$, $i = 1, \cdots, m$.

(4) The system

$$\left.\begin{aligned} &\frac{dx}{dt} = f(x) + g(x)u, \qquad x(0) = x_0 \\ &y_{A_i} = h_{A_i}(x), \quad i = 1, \cdots, m \end{aligned}\right\} \tag{3}$$

must be minimum-phase (has asymptotically-stable zero dynamics).

Finding auxiliary outputs

The auxiliary output maps $h_{A_1}(x), \cdots, h_{A_m}(x)$ are (Niemiec and Kravaris, 1998)

$$\begin{aligned} h_{A_1}(x) &= h_1(x) \\ &\vdots \\ h_{A_{m-1}}(x) &= h_{m-1}(x) \\ h_{A_m}(x) &= h_m(x) + \Sigma_{j=1}^{n-m} \lambda_j q_j(x) \end{aligned} \tag{4}$$

Here, the first $m-1$ auxiliary outputs are statically equivalent to the first $m-1$ process outputs by construction. The mth auxiliary output becomes statically equivalent to the mth process output when $q_1, \cdots, q_{n-m}$ vanish at the desired steady state. The constant parameters, $\lambda_1, \cdots, \lambda_{n-m}$ are adjusted such that the system of Eq. 3 is minimum-phase at the desired steady state; that is, $\lambda_1, \cdots, \lambda_{n-m}$ are adjusted to position the zeros of the linear approximation to Eq. 3 at desired locations $z_1^d, \cdots, z_{n-m}^d$ in the left-half plane.

Assuming that the $m \times m$ matrix

$$Q = \begin{bmatrix} [g_1(x)]_{n-m+1} & \cdots & [g_m(x)]_{n-m+1} \\ \vdots & \vdots & \vdots \\ [g_1(x)]_n & \cdots & [g_m(x)]_n \end{bmatrix}$$

is nonsingular, the scalar functions $q_1(x), \cdots, q_{n-m}(x)$ are constructed using

$$q_j(x) = [f(x)]_j - \{[g_1(x)]_j \cdots [g_m(x)]_j\} Q^{-1} \begin{bmatrix} [f(x)]_{n-m+1} \\ \vdots \\ [f(x)]_n \end{bmatrix}, \quad j = 1, \cdots, n-m \tag{5}$$

where $[g_i(x)]_j$ and $[f(x)]_j$ represent the jth rows of the vectors $[g_i(x)]$ and $f(x)$, respectively.

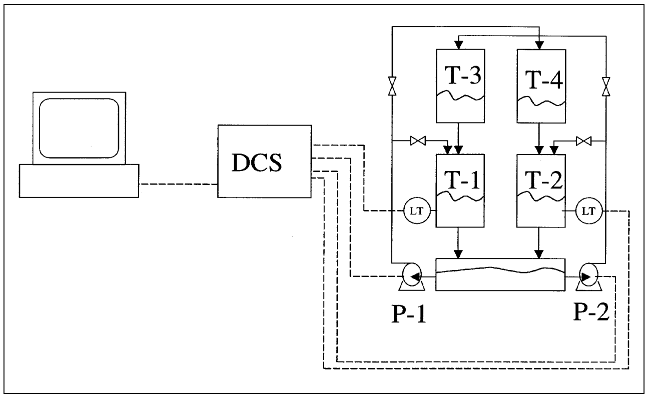

Figure 1. Liquid-level process.

Values of $\lambda_1, \cdots, \lambda_{n-m}$ that assign the zeros of the linear approximation to Eq. 3 at the desired steady state to z_j^d using the mapping in Eq. 4, are determined from

$$\det\begin{bmatrix} sI-A & -B \\ c_1 & 0 \\ \vdots & \vdots \\ c_{m-1} & 0 \\ c_{A_m} & 0 \end{bmatrix} = \det\begin{bmatrix} -A & -B \\ c_1 & 0 \\ \vdots & \vdots \\ c_{m-1} & 0 \\ c_m & 0 \end{bmatrix} \prod_{j=1}^{n-m}\left(1-\frac{s}{z_j^d}\right) \quad (6)$$

where $A = \partial f/\partial x|_{x_{ss}} + \sum_{j=1}^{m}[u_{ss}]_j\ \partial g_j/\partial x|_{x_{ss}}$, $B = g(x_{ss})$, $c_1 = \partial h_1/\partial x|_{x_{ss}}, \cdots, c_m = \partial h_m/\partial x|_{x_{ss}}$, $c_{A_m} = \partial h_{A_m}/\partial x|_{x_{ss}}$.

Pilot-Scale Liquid-Level Process

Figure 1 shows the four-tank system (Johansson and Nunes, 1998; Gatzke et al., 1999). Two centrifugal pumps P−1 and P−2 pump water from a basin into four overhead tanks, T−1, T−2, T−3, and T−4. Tanks T−3 and T−4 drain freely into tanks T−1 and T−2, which drain freely into the basin. The liquid levels in tanks T−1 and T−2 are measured with pressure transducers and, in each pump, the percentage of its maximum speed is manipulated. Below 32%, insufficient head is developed to induce flow into tanks T−3 and T−4. The piping is configured so that pumps P−1 and P−2 affect the levels in tanks T−1 and T−2, with a portion of the flow from P−1 (P−2) directly into tank T−1 (T−2). The remaining portion flows into T−4 (T−3), which drains into T−2 (T−1). The distributions of flow are set using the bypass valves. To introduce a disturbance, an artificial leak from tank T−3 to the basin is created using a submersible, on-off pump with a capacity of 32.21 cm^3/s. More details about the process can be found in Gatzke et al. (1999).

The computer is a PC with a 350 MHz processor, a 512 kB integrated cache, and 256 MB RAM. MATLAB and the Dynamic Data Exchange (DDE) software are installed on the computer. Once a control action is calculated by MATLAB using the control algorithms described next, with a sampling interval of 1 s, it is sent to a Bailey Freelance Distributed Control System (DCS) for implementation. The level signals are sampled and delivered to MATLAB using DDE software. When control is transferred from the DCS to MATLAB, the control algorithm is activated; that is, MATLAB simulates the closed-loop block diagram in SIMULINK. As the simulation proceeds, the calculated control action is implemented, with new output measurements sent to the controller. This is accomplished using the DDE commands.

Process model

A first-principles model of the process is used for controller synthesis (Johansson and Nunes, 1998; Gatzke et al., 1999). Under standard assumptions, mass balances on water in the four tanks yield

$$\begin{cases} \dfrac{dL_1}{dt} = -\dfrac{a_1}{A_1}\sqrt{2gL_1} + \dfrac{a_3}{A_1}\sqrt{2gL_3} + \dfrac{\gamma_1 k_1}{A_1}\upsilon_1 \\ \dfrac{dL_2}{dt} = -\dfrac{a_2}{A_2}\sqrt{2gL_2} + \dfrac{a_4}{A_2}\sqrt{2gL_4} + \dfrac{\gamma_2 k_2}{A_2}\upsilon_2 \\ \dfrac{dL_3}{dt} = -\dfrac{a_3}{A_3}\sqrt{2gL_3} + \dfrac{(1-\gamma_2)k_2}{A_3}\upsilon_2 \\ \dfrac{dL_4}{dt} = -\dfrac{a_4}{A_4}\sqrt{2gL_4} + \dfrac{(1-\gamma_1)k_1}{A_4}\upsilon_1 \end{cases} \quad (7)$$

Here, L_1, L_2, L_3 and L_4 are the liquid levels in tanks T−1 through T−4. υ_1 and υ_2 are the percentages of the maximum speed in pumps 1 and 2. They can vary between 32 and 100. A_1, A_2, A_3 and A_4 are the cross-sectional areas of tanks T−1 through T−4. a_1, a_2, a_3 and a_4 are the cross-sectional areas of the outlet pipes from tanks T−1 to T−4. g is the acceleration due to gravity. γ_1 is the fraction of the flow from pump P−1 that enters tank T−1, and γ_2 is the fraction of the flow from pump P−2 that enters tanks T−2. k_1 and k_2 are proportionality constants that relate the percentage of the maximum speed to the volumetric flow rates in pumps P−1 and P−2, respectively. The process parameter values are given in Table 1.

The steady-state pair (x_{ss}, u_{ss}) corresponding to $y_{sp} = [14.10\ 11.20]^T$ is ($L_{1_{ss}} = 14.10$, $L_{2_{ss}} = 11.20$ $L_{3_{ss}} = 7.18$, $L_{4_{ss}} = 4.66$, $\upsilon_{ss} = [59.76\ \ 59.90]^T$), which is hyperbolically stable (Jacobian of Eq. 7 has eigenvalues at $s = -0.017$, -0.021, -0.026 and -0.032, all in the left-half plane).

Table 1. Model Parameters

A_1, A_2, A_3, A_4 =	730 cm^2
a_1, a_2, a_3, a_4 =	2.3 cm^2
g =	981 $cm \cdot s^{-2}$
k_1 =	5.51 $cm^3 \cdot s^{-1}$
k_2 =	6.58 $cm^3 \cdot s^{-1}$
γ_1 =	0.333
γ_2 =	0.307

The zero dynamics are

$$\dot{\eta}_1 = -\frac{a_3}{A_3}\sqrt{2g\eta_1} + \frac{(1-\gamma_2)k_2}{A_3}\frac{A_2}{\gamma_2 k_2}\left(\frac{a_2}{A_2}\sqrt{2gy_{sp_2}} - \frac{a_4}{A_2}\sqrt{2g\eta_2}\right)$$

$$\dot{\eta}_2 = -\frac{a_4}{A_4}\sqrt{2g\eta_2} + \frac{(1-\gamma_1)k_1}{A_4}\frac{A_1}{\gamma_1 k_1}\left(\frac{a_1}{A_1}\sqrt{2gy_{sp_1}} - \frac{a_3}{A_1}\sqrt{2g\eta_1}\right)$$

whose Jacobian evaluated at $\eta_{ss} = [L_{3_{ss}}\ L_{4_{ss}}]^T = [7.18\ 4.66]^T$ has eigenvalues at $s = 0.033$ and -0.091. Since the first eigenvalue is in the right-half plane, the process is nonminimum-phase at this steady state. As a result, inverse responses to step changes in the manipulated inputs are present, as shown in Figure 2. Initially, L_1 decreases due to less flow into tank T−1 from pump P−1. Then, the increased flow from pump P−2 drains from tank T−3 into tank T−1, causing a net increase in the level of tank T−1. L_2 responds in a similar fashion (shows inverse response).

Controller Design

The process model Eq. 7 is in the form of Eq. 1 with

$$f(x) = \begin{bmatrix} -\frac{a_1}{A_1}\sqrt{2gx_1} + \frac{a_3}{A_1}\sqrt{2gx_3} \\ -\frac{a_2}{A_2}\sqrt{2gx_2} + \frac{a_4}{A_2}\sqrt{2gx_4} \\ -\frac{a_3}{A_3}\sqrt{2gx_3} \\ -\frac{a_4}{A_4}\sqrt{2gx_4} \end{bmatrix},$$

$$g(x) = \begin{bmatrix} \frac{\gamma_1 k_1}{A_1} & 0 \\ 0 & \frac{\gamma_2 k_2}{A_2} \\ 0 & \frac{(1-\gamma_2)k_2}{A_3} \\ \frac{(1-\gamma_1)k_1}{A_4} & 0 \end{bmatrix} \quad (8)$$

$$h_1(x) = x_1$$
$$h_2(x) = x_2$$

where $x = [L_1\ L_2\ L_3\ L_4]^T$, $u = [v_1\ v_2]^T$, $y = [L_1\ L_2]^T$, $m = 2$, $r_1 = r_2 = 1$, $u_{l_1} = u_{l_2} = 32$, and $u_{h_1} = u_{h_2} = 100$.

Controller I

Using the error-feedback control law presented by Kanter et al. (2002), a model-based controller is developed on the basis of the process outputs. With $p_1 = p_2 = 2$, the error-feedback controller has the form

$$\frac{dx_1}{dt} = -\frac{a_1}{A_1}\sqrt{2gx_1} + \frac{a_3}{A_1}\sqrt{2gx_3} + \frac{\gamma_1 k_1}{A_1}u_1, \quad x_1(0) = x_{1_0}$$

$$\frac{dx_2}{dt} = -\frac{a_2}{A_2}\sqrt{2gx_2} + \frac{a_4}{A_2}\sqrt{2gx_4} + \frac{\gamma_2 k_2}{A_2}u_2, \quad x_2(0) = x_{2_0}$$

$$\frac{dx_3}{dt} = -\frac{a_3}{A_3}\sqrt{2gx_3} + \frac{(1-\gamma_2)k_2}{A_3}u_2, \quad x_3(0) = x_{3_0}$$

$$\frac{dx_4}{dt} = -\frac{a_4}{A_4}\sqrt{2gx_4} + \frac{(1-\gamma_1)k_1}{A_4}u_1, \quad x_4(0) = x_{4_0}$$

$$u = \mathfrak{F}[x, e + h(x)] \quad (9)$$

where $u = \mathfrak{F}[x, \zeta]$ is the solution to the optimization problem

$$\min_u \sum_{i=1}^{m} w_i \left[\frac{\zeta_i - h_i(x) - 2\epsilon_i h_i^1(x,u)}{\epsilon_i^2} - h_i^2(x,u,0)\right]^2 \quad (10)$$

subject to the input constraints

$$u_{l_i} \le u_i \le u_{h_i}, \quad i = 1, \cdots, m$$

Here

$$h_1(x) = x_1$$

$$h_1^1(x,u) = -\frac{a_1}{A_1}\sqrt{2gx_1} + \frac{a_3}{A_1}\sqrt{2gx_3} + \frac{\gamma_1 k_1}{A_1}u_1$$

$$h_1^2(x,u,0) = -\frac{a_1}{A_1}\sqrt{2g}\frac{1}{2\sqrt{x_1}}\left[-\frac{a_1}{A_1}\sqrt{2gx_1} + \frac{a_3}{A_1}\sqrt{2gx_3} + \frac{\gamma_1 k_1}{A_1}u_1\right] + \frac{a_3}{A_1}\sqrt{2g}\frac{1}{2\sqrt{x_3}}\left[-\frac{a_3}{A_3}\sqrt{2gx_3} + \frac{(1-\gamma_2)k_2}{A_3}u_2\right]$$

$$h_2(x) = x_2$$

$$h_2^1(x,u) = -\frac{a_2}{A_2}\sqrt{2gx_2} + \frac{a_4}{A_2}\sqrt{2gx_4} + \frac{\gamma_2 k_2}{A_2}u_2$$

$$h_2^2(x,u,0) = -\frac{a_2}{A_2}\sqrt{2g}\frac{1}{2\sqrt{x_2}}\left[-\frac{a_2}{A_2}\sqrt{2gx_2} + \frac{a_4}{A_2}\sqrt{2gx_4} + \frac{\gamma_2 k_2}{A_2}u_2\right] + \frac{a_4}{A_2}\sqrt{2g}\frac{1}{2\sqrt{x_4}}\left[-\frac{a_4}{A_4}\sqrt{2gx_4} + \frac{(1-\gamma_1)k_1}{A_4}u_1\right]$$

and ϵ_1 and ϵ_2 are positive adjustable controller parameters that inversely affect the speed of the y_1 and y_2 responses, respectively.

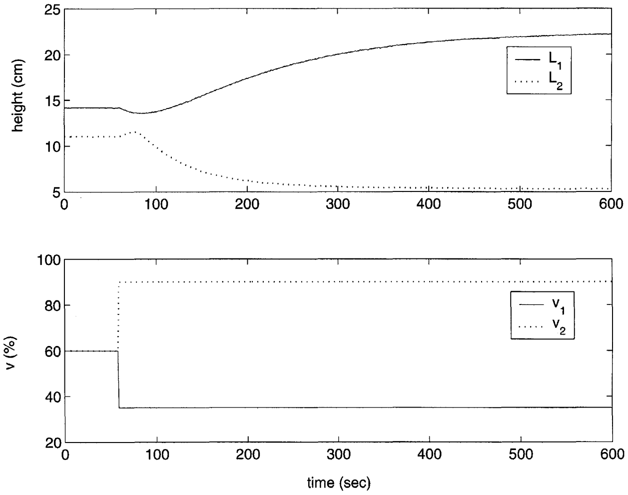

Figure 2. Real-time open-loop responses to step changes in the pump speeds.

Controller II

Alternatively, using the error-feedback control law presented in Kanter et al. (2002), a model-based controller is developed on the basis of auxiliary outputs obtained according to the procedure described earlier. The choices $z_1^d = -0.033$ and $z_2^d = -0.091$ lead to the auxiliary outputs

$$h_{A_1}(x) = h_1(x)$$
$$h_{A_2}(x) = h_2(x) - 37.35 q_1(x) + 37.34 q_2(x)$$
$$q_1(x) = -\frac{a_1}{A_1}\sqrt{2gx_1} + \frac{a_3}{A_1}\sqrt{2gx_3} + \frac{\gamma_1 a_4}{A_1(1-\gamma_1)}\sqrt{2gx_4}$$
$$q_2(x) = -\frac{a_2}{A_2}\sqrt{2gx_2} + \frac{a_4}{A_2}\sqrt{2gx_4} + \frac{\gamma_2 a_3}{A_2(1-\gamma_2)}\sqrt{2gx_3} \tag{11}$$

To derive the error-feedback control law, because the process with these auxiliary outputs is minimum-phase, it is sufficient to choose $p_1 = p_2 = r_1 = r_2 = 1$. The corresponding error-feedback control law has the form

$$\frac{dx_1}{dt} = -\frac{a_1}{A_1}\sqrt{2gx_1} + \frac{a_3}{A_1}\sqrt{2gx_3} + \frac{\gamma_1 k_1}{A_1}u_1, \quad x_1(0) = x_{1_0}$$
$$\frac{dx_2}{dt} = -\frac{a_2}{A_2}\sqrt{2gx_2} + \frac{a_4}{A_2}\sqrt{2gx_4} + \frac{\gamma_2 k_2}{A_2}u_2, \quad x_2(0) = x_{2_0}$$
$$\frac{dx_3}{dt} = -\frac{a_3}{A_3}\sqrt{2gx_3} + \frac{(1-\gamma_2)k_2}{A_3}u_2, \quad x_3(0) = x_{3_0}$$
$$\frac{dx_4}{dt} = -\frac{a_4}{A_4}\sqrt{2gx_4} + \frac{(1-\gamma_1)k_1}{A_4}u_1, \quad x_4(0) = x_{4_0}$$
$$u = \mathfrak{F}_A[x, e + h(x)] \tag{12}$$

where $u = \mathfrak{F}_A[x, \zeta]$ is the solution to the optimization problem

$$\min_u \sum_{i=1}^{m} w_i \left[\frac{\zeta_i - h_{A_i}(x)}{\epsilon_i} - h^1_{A_i}(x, u)\right]^2 \tag{13}$$

subject to the input constraints

$$u_{l_i} \le u_i \le u_{h_i}, \quad i = 1, \cdots, m$$

Here

$$h_{A_1}(x) = x_1$$
$$h^1_{A_1}(x, u) = -\frac{a_1}{A_1}\sqrt{2gx_1} + \frac{a_3}{A_1}\sqrt{2gx_3} + \frac{\gamma_1 k_1}{A_1}u_1$$
$$h_{A_2}(x) = h_2(x) - 37.35 q_1(x) + 37.34 q_2(x)$$
$$h^1_{A_2}(x, u) = L_f h_{A_2}(x) + L_{g_1} h_{A_2}(x) u_1 + L_{g_2} h_{A_2}(x) u_2$$

and ϵ_1 and ϵ_2 are positive adjustable controller parameters that inversely affect the speed of the y_1 and y_2 responses, respectively.

Controller tuning procedure

The following procedure is proposed for tuning the controllers:

- Using the conditions in Kanter et al. (2002) on the basis of the process model, choose the smallest values of the parameters p_1 and p_2, and the values of the parameters ϵ_1 and ϵ_2 (closed-loop "time constants" of the process output responses) that ensure closed-loop stability.
- In the presence of input constraints, using closed-loop simulation studies, the values of the parameters w_1 and w_2 are set to obtain satisfactory process output responses.
- In the presence of input constraints and in real-time, the parameters ϵ_1 and ϵ_2 are fine-tuned to obtain satisfactory process output responses.

This procedure led to the values: $\epsilon_1 = \epsilon_2 = 39.37$ s, $w_1 = w_2 = 10^6$, and $p_1 = p_2 = 2$ at $y_{sp} = [14.1\ 11.2]^T$ for Controller I, and $\epsilon_1 = \epsilon_2 = 50$ s and $w_1 = w_2 = 1$ for Controller II. Since Controller II has fewer tunable parameters than Controller I, it is easier to tune.

Controller Performance

With the process at the steady state corresponding to $y_{sp} = [11\ 19]^T$, the set point is adjusted to $y_{sp} = [14.1\ 11.2]^T$. The closed-loop responses under the two controllers are depicted in Figure 3, and the corresponding Integral of Squared Errors (ISEs) are given in Table 2. Under Controller I, the L_2 response has a significantly lower ISE, while the L_1 response has a slightly larger ISE. In terms of the sum of the ISEs (ISE1 + ISE2), Controller I performs better. Inverse response occurs in both controlled outputs under Controller I, but only L_2 experiences inverse response under Controller II. This is because (i) the first auxiliary output is identical to L_1 under Controller II's design and (ii) Controller II forces a first-order response to the first auxiliary output when the manipulated

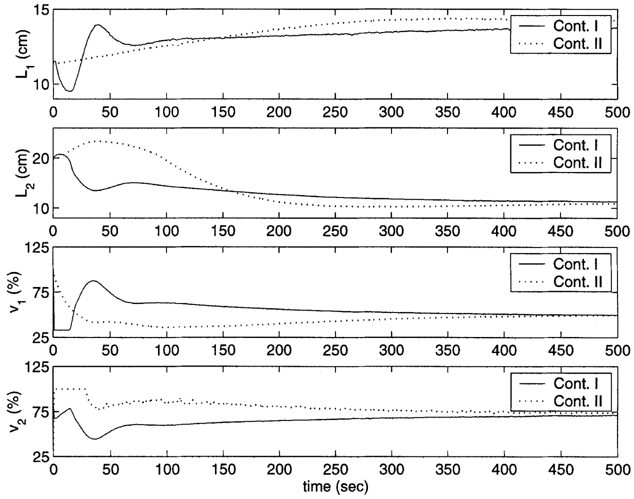

Figure 3. Real-time servo responses under Controllers I and II.

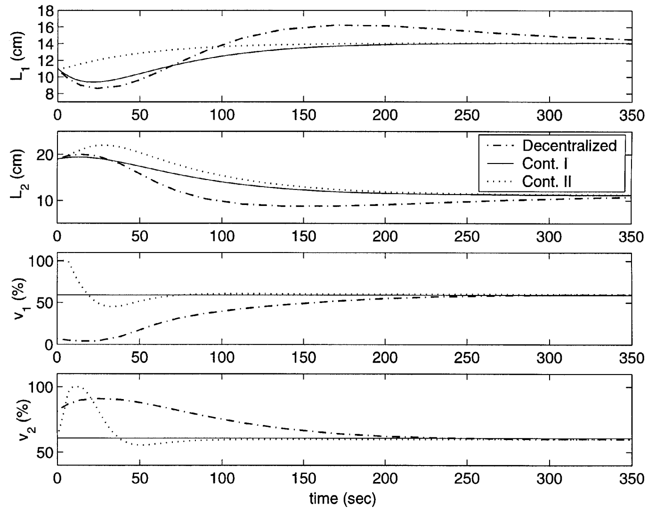

Figure 4. Simulated servo responses under the completely-decentralized linear controller and Controllers I and II.

inputs are no longer saturated. The price of the "inverse-free" response in L_1 is paid by L_2 which experiences a very large inverse response. Also, compared to the response under Controller II, the L_1 and L_2 responses under Controller I are more oscillatory. An attempt was made to increase the speed of the L_1 response by decreasing ϵ_1 in Controller I. However, sustained oscillations in the process outputs occurred before any significant increase in the speed of the L_1 response was observed. As expected, integral action of the controllers ensures offset-free responses in both controlled outputs. The real-time responses confirm the existing theoretical results (Holt and Morari, 1985; Niemiec and Kravaris, 1998); that is, inverse response in multivariable processes:

- Cannot be eliminated in all controlled outputs.
- Can be eliminated in real time in some controlled outputs at the expense of having larger inverse responses in other controlled outputs.

Figure 4 compares simulated servo responses under Controllers I and II and the completely-decentralized internal model controller

$$u_1(s) = \frac{s^2 + \alpha_1 s + \beta_1}{\gamma(\lambda^2 s^2 + 2\lambda s)} e_2(s)$$

$$u_2(s) = \frac{s^2 + \alpha_2 s + \beta_2}{\gamma(\lambda^2 s^2 + 2\lambda s)} e_1(s)$$

with $\alpha_1 = 0.05317$, $\beta_1 = 0.000674$, $\alpha_2 = 0.04462$, $\beta_2 = 0.0004839$, $\gamma = 0.0001627$, and $\lambda = 30$. The preceding completely-decentralized internal model controller consists of two single-input single-output (SISO), proportional-integral-derivative (PID) controllers with first-order low-pass filters. The controllers were designed and tuned using the standard internal model control guidelines. The details are as follows. Linear approximation of the process model around $y_{sp_1} = 14.1$ and $y_{sp_2} = 11.2$ leads to the process transfer function

$$G(s) = \begin{bmatrix} \dfrac{0.002513}{s + 0.01858} & \dfrac{0.0001627}{s^2 + 0.04462s + 0.0004839} \\ \dfrac{0.0001627}{s^2 + 0.05317s + 0.000674} & \dfrac{0.002767}{s + 0.02085} \end{bmatrix}$$

This matrix transfer function has a relative gain array of

$$\begin{bmatrix} -0.2840 & 1.2840 \\ 1.2840 & -0.2840 \end{bmatrix}$$

which suggests pairing (i) y_1 and u_2, and (ii) y_2 and u_1. The completely-decentralized internal model controller (two SISO PID controllers) are then designed using the process matrix transfer function. Although the process is mildly nonlinear, as Figure 4 shows clearly, Controllers I and II outperform the completely-decentralized linear control system in terms of servo performance. The response under the linear controller has the highest individual and sum of the ISEs.

Figure 5 shows the simulated output responses of the process to step and ramp changes in the set points [(a) step change and (b) ramp change]. The y_2 response under Controller I has a lower ISE in cases (a) and (b). However, y_1 response under Controller II has a lower ISE in cases (a) and (b). In terms of ISE, these responses are similar to those shown in Figures 3 and 4.

With the process at the steady state corresponding to $y_{sp} = [14.1\ 11.2]^T$, a step change is made in the leak from tank

Table 2. ISEs of the Responses

	Servo Responses		Regulatory Responses	
ISEs ($cm^2 \cdot s$)	Controller I	Controller II	Controller I	Controller II
ISE1 (ISE of L_1)	0.07e4	0.06e4	5.21e2	0.68e2
ISE2 (ISE of L_2)	0.31e4	1.36e4	0.53e2	5.23e2
ISE1 + ISE2	0.38e4	1.42e4	5.74e2	5.91e2

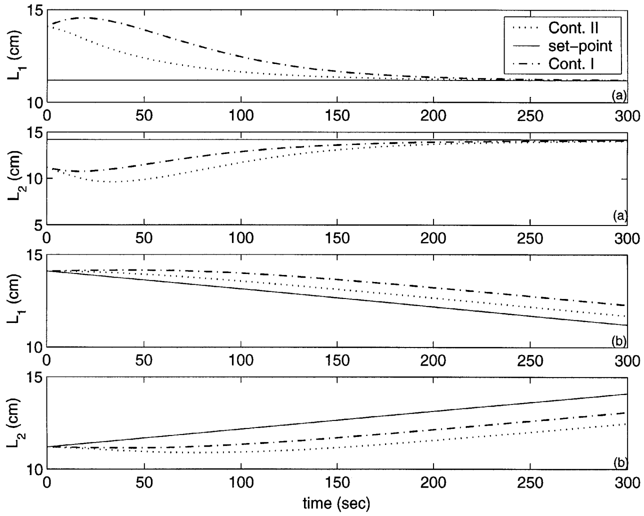

Figure 5. Simulated servo responses under Controllers I and II, with (a) step- and (b) ramp-changes in the set points.

T−3 (an unmeasured disturbance) from 0 to 32.21 cm^3/s at $t = 10$ s. The closed-loop responses under the two controllers are depicted in Figure 6, and the corresponding ISEs are given Table 2. As in the servo responses shown in Figure 3, under Controller I, the L_2 response has a lower ISE, while the L_1 response has a larger ISE. The price of the response with lower ISE in L_1 under Controller II is paid by the higher ISE of the L_2 response. In terms of the sum of the ISEs (ISE1 + ISE2), the performances of the two controllers are comparable. The integral actions of the controllers reject the effects of the constant unmeasurable disturbance and possible model errors.

Conclusions

Real-time implementation of a recently-developed method of model-based controller design was presented. In particular, the performance of two controllers were studied. Controller I was designed on the basis of the actual process outputs, while Controller II was designed on the basis of two auxiliary outputs. Controllers I and II showed similar performance in terms of the sum of the ISEs. Among the advantages of using auxiliary outputs instead of the actual process outputs for the controller design were that: (i) all of the inverse response was moved to one output, resulting in better servo performance in the remaining output; (ii) slightly less computation time was required to compute u; and (iii) the controller tuning was easier.

In general, a controller designed on the basis of the auxiliary outputs requires less computation time than one designed on the basis of actual process outputs. When auxiliary outputs are used, the objective function of the controller is more likely to be convex, and, hence, simpler algorithms, such as the one described in Soroush and Valluri (1999), are adequate. In the case of a nonconvex controller performance index, a global optimization algorithm is necessary, greatly increasing the computation time. Because of its low computational load, an auxiliary-output-based controller is more suitable for fast processes, such as mechanical and electrical processes. For the four-tank process, Controllers I and II both have convex objective functions. As a result, their computational speeds do not differ significantly.

Nonminimum-phase behavior can be due to the presence of an unstable mode in the zero dynamics of the process (finite right-half-plane zero in the linear case) and/or a time delay (infinite right-half-plane zero in the linear case). The real-time results "validated" the existing theoretical proofs that inverse response (caused by unstable zero dynamics) in a multivariable process:

- Cannot be eliminated in all controlled outputs.
- Can be eliminated in some controlled outputs at the expense of having larger inverse responses in other controlled outputs.

Thus, as already shown theoretically in the literature (Holt and Morari, 1985; Niemiec and Kravaris, 1998), a model-based controller: (i) can eliminate nonminimum-phase behavior in a controlled output if the behavior is caused by unstable zero dynamics (finite right-half-plane zero in the linear case); (ii) cannot eliminate the behavior, if it is caused by a time delay (infinite right-half-plane zero in the linear case). Nonminimum-phase response caused by a time delay cannot be eliminated by control, because the elimination requires a noncausal controller.

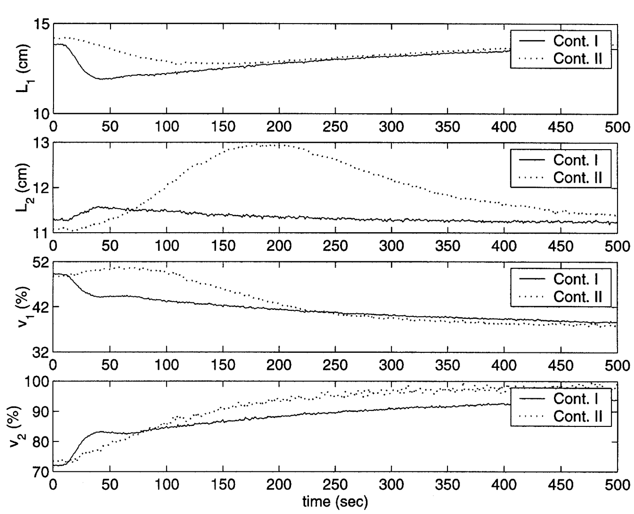

Figure 6. Real-time regulatory responses under Controllers I and II.

Acknowledgments

The authors extend their thanks to Frank J. Doyle III for facilitating the authors' use of his laboratory and Nick Hernjak for assisting in operating the liquid-level process. The first and second authors gratefully acknowledge partial support from the National Science Foundation through grant CTS-0101237. The third author would like to acknowledge financial support from the National Science Foundation through grant CTS-0101133.

Notation

a_1, a_2, a_3, a_4 = outlet cross-sectional area of tanks T−1 to T−4, cm^2

A_1, A_2, A_3, A_4 = cross-sectional area of tanks T−1 to T−4, cm^2

A = Jacobian matrix of Eq. 3
B = B-matrix of linear approximation of Eq. 3
e = error in measured output vector, $y_{sp} - \bar{y}$
g = acceleration due to gravity, $cm \cdot s^{-2}$
$h_i(.)$ = ith output map
$h_{A_i}(.)$ = ith auxiliary output map
I = identity matrix
k_1, k_2 = pump constants, $cm^3 \cdot s^{-1}$
L_1, L_2, L_3, L_4 = level in tanks 1 to 4, m
m = number of inputs and outputs
n = process order
p_i = orders of the requested response for y_i
P−1, P−2 = pumps 1 and 2
$q_1(x), \cdots, q_{n-m}(x)$ = functions that vanish at steady state; see Eq. 5
Q = last m rows of $g(.)$
r_i = relative order of y_i
t = time, s
T−1, T−2, T−3, T−4 = tanks 1, 2, 3 and 4
u = process input vector
u_{l_i} = lower bound on ith process input
u_{h_i} = upper bound on ith process input
v_1, v_2 = percent of maximum speed in pumps 1 and 2
w_i = ith weight in the controller performance index
x = vector of state variables
y = controlled output vector
y_A = auxiliary output vector
$\bar{y}$ = measured output vector
y_{sp} = set point vector
$z_1^d, \cdots, z_{n-m}^d$ = desired locations of the zeros of linear approximation of process with equivalent outputs

Greek letters

γ_1 (γ_2) = fraction of flow leaving pump P−1 (pump P−2) that enters tank T−1 (tank T−2)
ϵ_i = ith tunable parameter of controller
$\zeta_i = e_i + h_i(x)$
η = states of zero dynamics, $\eta_1 = L_3$, $\eta_2 = L_4$
$\lambda_1, \cdots, \lambda_{n-m}$ = parameters in h_{A_m} that place zeros of Eq. 3 at $z_1^d, \cdots, z_{n-m}^d$

Subscripts

A = auxiliary
ss = steady state
sp = set-point
0 = initial value
$[.]_i$ = ith row of matrix

Literature Cited

Chen, D., and B. Paden, “Stable Inversion of Nonlinear Non-minimum-phase Systems,” *Int. J. Contr.*, **64**, 81 (1996).

Chen, H., and F. Allgower, “A Quasi-infinite Horizon Nonlinear Model Predictive Control Scheme with Guaranteed Stability,” *Automatica*, **34**, 1205 (1998).

Devasia, S., “Approximated Stable Inversion for Nonlinear Systems with Nonhyperbolic Internal Dynamics,” *IEEE Trans. on Automatic Contr.*, **44**, 1419 (1999).

Devasia, S., D. Chen, and B. Paden, “Nonlinear Inversion-based Output Tracking,” *IEEE Trans. on Automatic Contr.*, **41**, 930 (1996).

De Nicolao, G., L. Magni, and R. Scattolini, “Stabilizing Receding-Horizon Control of Nonlinear Time-Varying Systems,” *IEEE Trans. on Automatic Control*, **43**, 1030 (1998).

Doyle III, F. J., F. Allgöwer, and M. Morari, “A Normal Form Approach to Approximate Input-Output Linearization for Maximum Phase Nonlinear SISO Systems,” *IEEE Trans. on Automatic Control*, **41**, 305 (1996).

Gatzke, E. P., R. Vadigepalli, E. S. Meadows, and F. J. Doyle III, “Experiences with an Experimental Project in a Graduate Control Course,” *Chem. Eng. Educ.*, **33**, 270 (1999).

Holt, B. R., and M. Morari, “Design of Resilience Processing Plants—VI: The Effect of Right Half-Plane Zeros on Dynamic Resilience,” *Chem. Eng. Sci.*, **40**, 59 (1985).

Hunt, L. R., and G. Meyer, “Stable Inversion for Nonlinear Systems,” *Automatica*, **33**, 1549 (1997).

Isidori, A., *Nonlinear Control Systems*, Springer-Verlag, New York (1995).

Isidori, A., and A. Astolfi, “Disturbance Attenuation and H_∞ Control via Measurement Feedback in Nonlinear Systems,” *IEEE Trans. on Automatic Contr.*, **37**, 1283 (1992).

Isidori, A., and C. I. Byrnes, “Output Regulation of Nonlinear Systems,” *IEEE Trans. on Automatic Contr.*, **35**, 131 (1990).

Johansson, K. H., and J. L. R. Nunes, “A Multivariable Laboratory Process with an Adjustable Zero,” *Proc. of American Contr. Conf.*, Philadelphia, PA, Omnipress, Madison, WI, p. 2045 (1998).

Kanter, J. M., M. Soroush, and W. D. Seider, “Nonlinear Controller Design for Input-Constrained, Multivariable Processes,” *I&EC Res.*, **41**, 3735 (2002).

Kravaris, C., and P. Daoutidis, “Nonlinear State Feedback Control of Second-Order Non-minimum Phase Nonlinear Systems,” *Comp. Chem. Eng.*, **14**, 439 (1990).

Kravaris, C., M. Niemiec, R. Berber, and C. B. Brosilow, “Nonlinear Model-based Control of Nominimum-phase Processes,” *Nonlinear Model Based Process Control*, R. Berber and C. Kravaris, eds., Kluwer, Dordrecht, The Netherlands (1998).

McLain, R. B., M. J. Kurtz, M. A. Henson, and F. J. Doyle III, “Habituating Control for Nonsquare Nonlinear Processes,” *Ind. Eng. Chem. Res.*, **35**, 4067 (1996).

Niemiec, M., and C. Kravaris, “Controller Synthesis For Multivariable Nonlinear Non-minimum-phase Processes,” *Proc. of American Contr. Conf.*, Philadelphia, PA, Omnipress, Madison, WI, 2076 (1998).

Soroush, M., and S. Valluri, “Optimal Directionality Compensation in Processes with Input Saturation Non-linearities,” *Int. J. Control*, **72**, 1555 (1999).

van der Schaft, A. J., “L_2 Gain Analysis of Nonlinear Systems and Nonlinear State Feedback H_∞ Control,” *IEEE Trans. on Automatic Contr.*, **37**, 770 (1992).

Wright, R. A., and C. Kravaris, “Non-Minimum-Phase Compensation for Nonlinear Processes,” *AIChE J.*, **38**, 26 (1992).

Manuscript received Aug. 23, 2001, and revision received May 21, 2002.